Astron. Astrophys. 326, 528–536 (1997)

ASTRONOMY AND ASTROPHYSICS

# Blue stars in the center of the S0 galaxy NGC 5102⋆

**J.-M. Deharveng**[1], **R. Jedrzejewski**[2], **P. Crane**[3], **M.J. Disney**[4], **and B. Rocca-Volmerange**[5]

[1] Laboratoire d'Astronomie Spatiale du CNRS, Traverse du Siphon, BP 8, F-13376 Marseille Cedex 12, France
[2] Space Telescope Science Institute, 3700 San Martin Drive, Baltimore, MD 21218, USA
[3] European Southern Observatory, Karl Schwarzschild Strasse 2, D-8046 Garching, Germany
[4] Department of Physics and Astronomy, University of Wales College of Cardiff, P.O. Box 913, Cardiff CF2 3YB, UK
[5] Institut d'Astrophysique, 98bis Boulevard Arago, F-75014 Paris, France

Received 7 March 1997 / Accepted 22 April 1997

**Abstract.** The S0 galaxy NGC 5102 has been observed with the Faint Object Camera on-board the *Hubble Space Telescope*. Individual blue stars have been resolved in the central region and measured photometrically through the F175W and F342w filters. The limits of detection and completeness are not uniform over the field observed because the unresolved galaxy light increases toward the center. Comparison of integrated light with previous IUE observations and study of the light profiles determined from the FOC images confirm the blue color gradient inward. The F175w−F342w color is found to get bluer from 1.″4 (21 pc) to 0.″4 (6 pc) but the gradient does not continue in the nucleus. There is no evidence for a central core. The resolved blue stars are slightly more concentrated toward the center than the integrated light distribution. In the $m_{175}$ vs. $m_{175}-m_{342}$ plane the stars are at positions where either young stars or P-AGB stars may be expected. Although neither interpretation is certain, several arguments suggest that the majority of the resolved stars are young and belong to the last generation of a star formation episode that ended ∼15 Myr ago. According to spectral evolution models, the IUE ultraviolet spectrum is best reproduced if this star formation episode started 500–800 Myr ago.

**Key words:** galaxies: evolution – galaxies: individual: NGC 5102 – galaxies: elliptical and lenticular – galaxies: stellar content – ultraviolet: galaxies

## 1. Introduction

NGC 5102 is a blue and gas-rich S0 galaxy that has attracted attention because of a blue color gradient in its center (van den Bergh 1976, Pritchet 1979) and an unusual ultraviolet spectrum (Rocca-Volmerange & Guiderdoni 1987, Burstein et al. 1988). Both characteristics have been interpreted as evidence for recent star formation activity in the central region. Signs of low-level star formation had also been reported in the outer regions (van den Bergh 1976). Van Woerden et al. (1993) have studied the distribution and the motions of atomic hydrogen while summarizing the optical, X-ray and infrared properties. Mc Millan, Ciardullo & Jacoby (1994) recently investigated the distribution of ionized gas and identified a number of planetary nebulae.

This paper reports the first direct detection of individual blue stars in the central region of NGC 5102. These stars are resolved with the Faint Object Camera (FOC) on board the *Hubble Space Telescope*. In addition to confirming the interpretation of the abnormal blue and UV colors, our motivation was to characterize the star formation phenomenon in an old population and possibly to understand why such a phenomenon has occurred in NGC 5102. Beyond the specific example of NGC 5102, we wished to pursue the broader issues of residual star formation in early-type galaxies, under which conditions it may happen and how, observationally, it may be distinguished from the extreme horizontal branch stars and their evolutionary progeny that are now recognized as the dominant contributors to the UV emission from early-type galaxies (e.g. Greggio & Renzini 1990, Dorman et al. 1993, Dorman et al. 1995, Ferguson et al. 1991, Ferguson & Davidsen 1993, Brown et al. 1995).

## 2. Observations and data reduction

NGC 5102 was observed on 1995 May 26, using the 512×512 pixel imaging mode (pixel size 0.″01435×0.″01435, field of view 7.″3×7.″3) of the f/96 camera of the COSTAR-corrected FOC (Jedrzejewski et al. 1994). Several exposures were taken using the broad-band filters F175W and F342W, centered at wavelengths of 1730 and 3410 Å and of FWHM 716 and 702 Å, respectively. The ultraviolet filter suffers from non-negligible red leak (transmission of a few $10^{-4}$ in the visible). In anticipation of saturation effects in the F342W image, one exposure (769 s) was taken with 4 mag of neutral density filter (F342W+F4ND).

*Send offprint requests to*: J.-M. Deharveng

⋆ Based on observations with the NASA/ESA Hubble Space Telescope, obtained at the Space Telescope Science Institute, which is operated by AURA, Inc., under NASA contract NAS 5-26555.

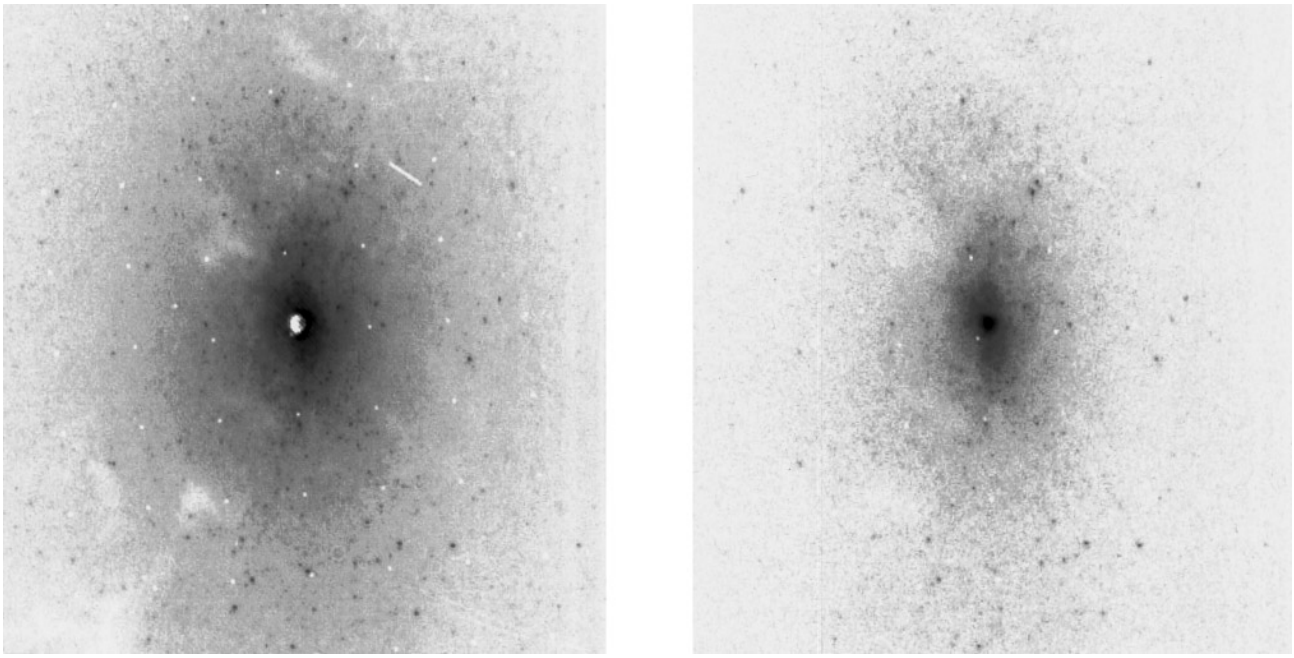

**Fig. 1.** Greyscale representation of the F342W (left) and F175W (right) summed images of the central region of NGC 5102. The images are displayed on a logarithmic scale. The field of view in each image is $7\farcs3 \times 7\farcs3$, and North is inclined at 45°to the vertical, with East pointing to the left. This makes the (optical) major axis (position angle of 48°) almost vertical. The regular pattern of dots is due to the reseau marks etched onto the FOC photocathode, which are used for geometric registration of the images. The central regions of the F342W image are heavily saturated, so the intensity distribution appears to have a "hole" in the center.

All images were taken in FINE LOCK mode. The data were automatically processed and calibrated by the Routine Science Data Processing system. The images obtained with the same filter were found to be aligned to within a fraction of pixel and therefore were co-added. This left us with total exposure times of 4075 s for the F175W image and 1789 s for the F342W image.

The final co-added F175W and F342W images are displayed in Fig. 1 and show a sizable number of resolved point-like sources over the diffuse bulge light. The FWHM of these sources ($\sim 0\farcs03$) as well as the photometry discussed in the next section allow their identification as stars in the galaxy NGC 5102. These stars contrast better in the outer parts where the underlying galaxy light is fainter. In the corners of the F175W image the count rate is of the order of $0.9 \times 10^{-3}$ count/pixel/s and may still include a small contribution from the galaxy light as shown by comparison with the typical value of $0.7 \times 10^{-3}$ count/pixel/s reported in the instrument handbook (Nota et al. 1995) and actually found at the edge of the exposure with the neutral density filter (where the galaxy contribution is negligible). In the F342W image the contribution from the unresolved galaxy light remains dominant over the dark count rate at the edge of the field. Both images reveal several dust patches.

## 3. Analysis

### *3.1. Photometry of the resolved stars*

Since the crowding is not severe, stellar fluxes can be measured using the standard aperture photometry package *apphot* of IRAF, by following the method of Paresce et al. (1995). The main difficulty here comes from the unresolved galaxy light which increases by a factor of more than 20 from the edge of our field to the inner bulge and does not allow to maintain simultaneously the same significance of detection and the same limiting magnitude over the entire field of view. Subtracting an image obtained by smoothing the light distribution can help the visual identification of point source objects but does not change the fact that the magnitude of the fluctuations increases toward the center, as the average flux level increases. In order to keep a relatively homogeneous significance of star detection (at the expense of an uniform limiting magnitude), we have run the *daofind* star finding routine with different threshold values. To this end we have divided the image in four domains in which it is reasonable to have a constant threshold value. We have set this threshold at approximately 6 $\sigma$ above the average sky level. These domains are defined by elliptical contours with semi-major axis $2\farcs3$, $1\farcs4$, $0\farcs57$ and axis ratio 0.7, 0.58, 0.5 respectively. The procedure was run on the F175W image and the list of detected stars that we obtained was used for aperture photometry in both images.

The magnitudes $m_{175}$ and $m_{342}$ of each star were calculated as

$$m = -2.5 \log \frac{I\,c}{\epsilon\,t} - 21.1$$

where $I$ is the inverse sensitivity of the modes used ($7.65 \times 10^{-17}$ and $3.50 \times 10^{-18}$ ergs cm$^{-2}$ s$^{-1}$ Å$^{-1}$ per count/s respectively for the F175W and F342W frames), $c$ is the total number

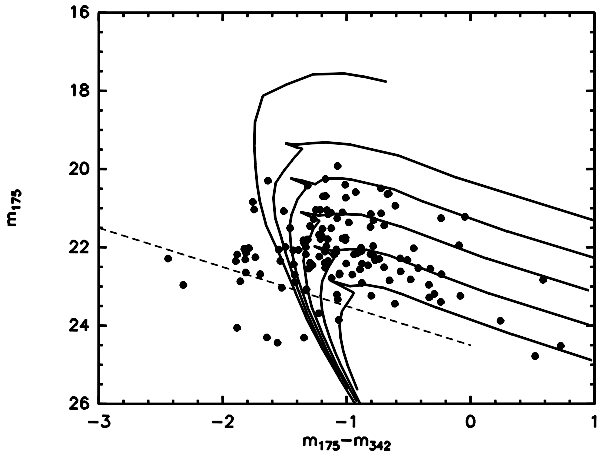


**Fig. 2.** Color-magnitude diagram obtained from the magnitudes measured on the summed F175W and F342W images. The dashed line shows the detection limit in the F342W image. The solid lines show the isochrones of Bertelli et al. for the ages log t = 6.6, 7.0, 7.2, 7.4, 7.6, 7.8 years (from top to bottom).

of counts attributable to the star, $t$ the exposure time in s and $\epsilon$ the energy fraction associated with the aperture photometry. The latter factor accounts for the amount of light missed by the aperture as well as unduly subtracted out in the background reference annulus. We have adopted an aperture radius of 3 pixels and a reference annulus with inner and outer radii of 4 and 7 pixels, respectively. We have measured $\epsilon_{175}$ = 0.48 and $\epsilon_{342}$ = 0.59 with available PSF images. A total of 130 stars, measured in both images (we have discarded a few measurements as discussed later), are displayed in the color-magnitude diagram (CMD) of Fig. 2 obtained by plotting the observed $m_{175}$ magnitude versus the $m_{175}-m_{342}$ color.

The statistical and systematic uncertainties expected in the FOC images analysed with the aperture photometry technique have been discussed by Paresce et al. (1995). In our case the uncertainty due to the absolute calibration should be slightly increased over the quoted value of 15% because the energy fraction factor could not be verified very accurately in our image and a nominal value was adopted. It should be noted that the color term is less affected by this additional source of error. The statistical uncertainty associated with the aperture photometry measurement and returned by the *phot* package is $\sim \pm 0.1$ and $\sim \pm 0.04$ at 22 mag with the F175W and F342W filters, respectively. This uncertainty increases at fainter magnitudes and in areas of large background from the galaxy light.

The completeness in our sample is a severe issue because it is not only a function of magnitude but also a function of the surface brightness of the background galaxy light. This is especially true for studying the distribution of the individual stars. As a first approximation, we have evaluated the incompleteness in each domain defined above where the limit of detection is expected to be reasonably uniform. Practically, we have added artificial stars at random places in our image and repeated our finding operation for several trials at different magnitudes. We find in this way that our photometry is 95% complete at $m_{175}$ = 22.5, 28% at $m_{175}$ = 23 in the outer domain where the detection is the deepest. In the second domain (the outer domain is the first and we move to the center) the completeness fractions decrease to 66% and 7% (for respectively the same magnitudes as before), then we obtain 78% at $m_{175}$ = 21.5, 30% at $m_{175}$ = 22 in the third domain. No realistic evaluation was made in our central domain.

The F175W image has been used to set the detection limit of the sample because it allows the selection of the hottest stars and it was less deep than the F342W image. As a consequence of the latter, faint stars are seen in the F342W image that have no counterpart in the F175W frame. These stars are red and have no impact on the completeness of our sample. On the blue side of the CMD (in Fig. 2) we have plotted the (dashed) line resulting from the detection limit in the F342W frame (scaled down according to the sensitivity difference from the detection limit in the F175W frame). The F342W image is deep enough that all stars above the detection limit in the F175W image with realistic blue colors are detected. In order to check this, we have visually examined three stars that were not detected in the F342W frame and two objects with abnormally blue color. We have found that their detection was already marginal in the F175W frame; the two latter objects have been discarded.

### *3.2. Galaxy light distribution*

As noted above, individual stars are resolved in both images against the diffuse light of the integrated stellar population of the bulge. The contribution of the resolved stars to the total light is minimal (of the order of 2 to 3 percent), implying that we are only resolving the tip of the blue stellar population. For all practical purposes the study of the unresolved stellar population is equivalent to that of the total light. This allows direct comparison with previous photometric data based on integrated light and avoids painful completeness corrections for removing the contribution of resolved stars down to a given magnitude.

We have first calculated the total number of counts due to galaxy light in the field of view. In order to avoid the warped edges of the images, the calculation was made in a circular aperture of radius 220 pixels, i.e. 3″.16 and an area of 31.3 square arcsec. For the F175W co-added images we get a total count rate of 280 count/s (after subtracting a detector background of $7 \times 10^{-4}$ count/pixel/s). Only a fraction of these are due to true UV light because of the F175W filter red leak. In order to determine this fraction and to make comparison with previous IUE measurements (Burstein et al. 1988), we need to use a spectrum of the galaxy. For a reasonable approximation we extend the IUE spectrum into the visible with a model spectral energy distribution (see Sect. 4.2) that we have normalized to a magnitude V = 11.94 in the equivalent IUE aperture of 154 square arcsec (Burstein et al. 1988). Assuming that the spectral shape is the same in the area of 31.3 square arcsec, we scale down the spectral energy distribution by a factor of 1.84 according to the aperture photometry of van den Bergh (1976) in V light. By synthetic photometry using the synphot package we predict 160

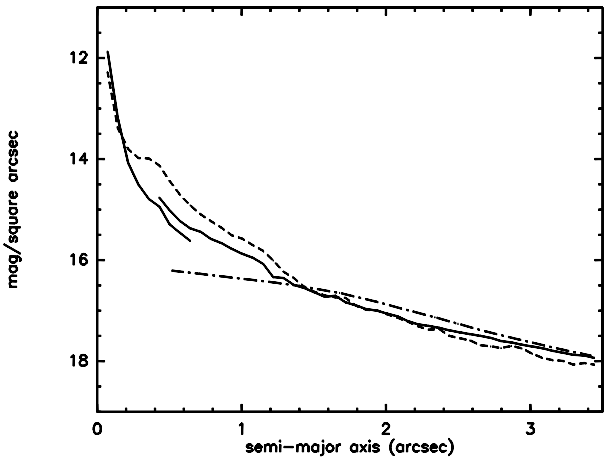


**Fig. 3.** Comparison of the average radial light profiles resulting from isophote fitting: F342W, solid lines (there are two curves because the image with the neutral density filters has been used for the central region); F175W, dashed line (in the outer part the profile is very depending on the correction for detector background). The dot-dashed line is the B-luminosity profile from Pritchet (1979). At the distance of NGC 5102 1″ is ∼ 15 pc.

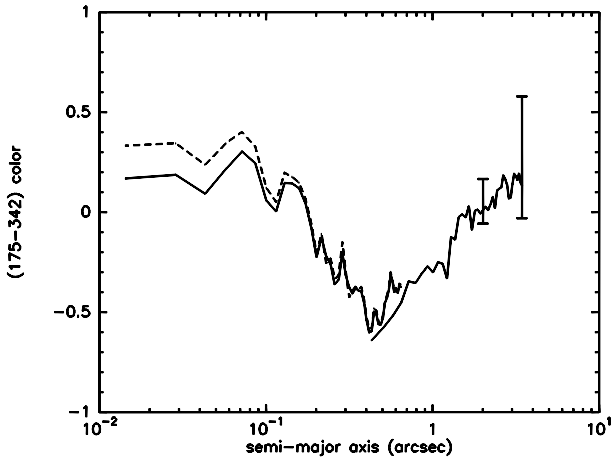


**Fig. 4.** The average (175-342) color profile resulting from isophotal fitting as in Fig. 3. The log scale for the distance emphasizes the very central region. At the distance of NGC 5102 1″ is ∼ 15 pc and a pixel is ∼ 0.2 pc. The wrinkles are due to the noise accompanying isophotal fitting with steps as small as 1 pixel in the central regions. The F342W image with the neutral density filter is used in the central region. The dashed line is the color variation without the correction for non-linearity effects in the F175W image. The error bars show the uncertainty at the edge of the field resulting from dark current subtraction (upper bound $0.9\times10^{-3}$ count/pixel/s; lower bound $0.6\times10^{-3}$ count/pixel/s).

count/s whereas we get 280 count/s. This contradiction cannot be explained alone by a possible underestimation of the detector background ($9 \times 10^{-4}$ count/pixel/s is possible instead of $7 \times 10^{-4}$ count/pixel/s). It probably tells us that the scaling factor based on the V light profile is not appropriate for the UV and suggests a color gradient between the UV and the visible in the domain covered by the two apertures we refer to (radius of 3.″1 used in the FOC image and equivalent radius of 7″ for the IUE diaphragm), in the sense of the central region getting bluer. A bluer nucleus has also been reported by van den Bergh (1976) and Pritchet (1979). Our conclusion is however affected by the uncertainties accompanying the approximation of the spectral energy distribution and the comparison of aperture photometry with different instruments (orientation and shape of apertures). Assuming that our approximation of the spectrum is valid for the purpose of red leak calculation, synthetic photometry shows that only 75% of the counts are due to true UV light, i.e. below 2400 Å.

In order to reduce some of the above uncertainties and to take advantage of the angular resolution of the HST, we have concentrated on the study of a possible color gradient within the images themselves. Average light profiles have been calculated by fitting elliptical isophotes with the IRAF/STSDAS task *ellipse* and have been plotted in Fig. 3 (1″ corresponds to 15 pc and 1 pixel to 0.2 pc in NGC 5102). The profile in F342W light is obtained with the co-added images using radii from 30 pixels to 240 pixels and with the image obtained with neutral density filters for radii from 5 to 45 pixels; the agreement looks reasonable in the regime of overlap. The profile in F175W light has been plotted assuming the nominal detector dark current of $7 \times 10^{-4}$ count/pixel/s; it would be of course steeper in the outer part if more of the count rate is ascribed to detector background. In Fig. 4 we directly display the $m_{175}-m_{342}$ color variation while emphasizing the very central region. From 1.″4 outward, the observed profiles are comparable to the profile in B-light from Pritchet (1979) and reveal a shallow color gradient (getting redder outward) consistent with the gradient inferred from our comparison above with the IUE measurements and the U−B gradient reported by van den Bergh (1976). A quantitative comparison is not possible given the uncertainties of our dark current subtraction and the fact that ground-based photometry was made through large diaphragms. From 1.″4 inward, the $m_{175}-m_{342}$ blue color gradient gets much steeper (from $m_{175}-m_{342} \sim 0.0$ at 1.″4 to $\sim -0.5$ at 0.″4) but does not extend into the very center where the color gets back to ∼0.2, a value comparable to that typically found at about 3″ from the center. We have performed a correction for non-linearity effects in the F175W image due to the high count rates in the central regions of the galaxy and Fig. 4 shows the impact of this correction on the color. Although this correction is uncertain, it cannot explain the upturn of the color gradient in the very center: at 0.″2 from the center the count rate is already less than 0.1 count $s^{-1}$. From the brightness profiles in the very center (Fig. 5) there is no evidence for a core and NGC 5102 falls into the category of galaxies that have profiles that continue into the resolution limit as steep power laws (Lauer et al. 1995).

### *3.3. The spatial distribution of resolved stars*

Examination of Fig. 1 shows that the individual stars are preferentially found in the direction of the galaxy major axis (almost the vertical in Fig. 1). This visual impression has been quanti-

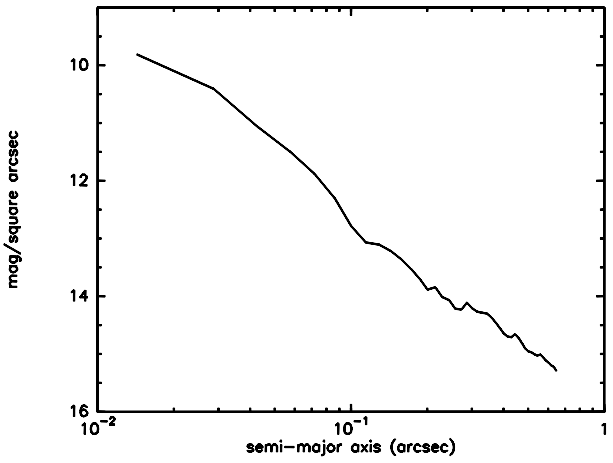


**Fig. 5.** Same as Fig. 3 with only the F342W (plus neutral filter) average radial light profile and the log scale emphasizing the central region.

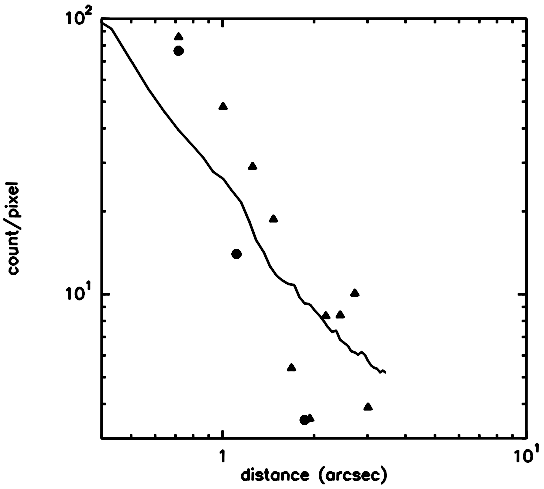


**Fig. 6.** Comparison of the surface density of resolved stars ($m < 21.75$) with the UV light radial profile. The surface density is in arbitrary units. The light profile results from ellipse fitting and is expressed in count/pixel. The distance along x-axis is the semi-major axis distance for the light profile, the distance from the center of the galaxy for stars within 15°of the major axis (circle), the radial distance of the stars calculated in a disk of inclination angle 30° (triangle).

tatively confirmed by counting the stars as a function of position angle, using 10° wide angular bins with the center of the galaxy as the summit. With stars in our two external domains only, we find that the direction favoured is at a position angle of 10°±10 from vertical, i.e. 55° from North and close to the major axis of the galaxy (optical and HI axis, respectively 48° and 43° from North, as reported by van Woerden et al. 1993). This approach is not severely affected by the photometric incompleteness; if these effects are further reduced by considering only stars brighter than 22 mag, the result is affected by small number statistics but not basically changed.

Whether the resolved blue stars follow the overall galaxy light distribution is more difficult to answer, especially since the detection limit and the completeness are depending on this background light. In a first approach we have tried to stay as consistent as possible with our analysis of the completeness; we have counted stars in our three external domains, corrected these numbers for incompleteness according to the magnitude range of the stars and compared the resulting numbers with the integrated light in the same domains. We find that the number of stars is in direct proportion to the integrated light in the two external domains but we find slightly more stars closer to the center than one would expect from the integrated light. As this approach is limited to a comparison between two series of only three numbers, we have attempted a comparison of the surface density of resolved stars with the radial light profile obtained as a function of the equivalent semi-major axis (see previous section). Because the incompleteness is more difficult to account for in this approach, we limit ourselves to stars brighter than 21.75 mag. The comparison can be made either with a limited number of stars close to the major axis (±15°) or with all the stars assuming that they are in a disk and their surface density calculated therein adopting an inclination angle of 30°. Both comparisons are displayed in Fig. 6. Within the limits of completeness, small number statistics and the lack of investigation in the inner 40 pixels (0.″6), Fig. 6 shows that the spatial distribution of resolved stars follows the galaxy light distribution with the stars being slightly more concentrated. This concentration seems even more dramatic with the brightest stars in the sense that no stars with $m_{175} < 21$ are observed in the outer parts but an effect from small-number statistics cannot be excluded. A similar result would be obtained with an angle of 70°, perhaps indicating that a disk structure is not required by the data. Another feature of the distribution of resolved stars is the absence of clustering as usually found in spiral arms of late-type galaxies and star-forming galaxies. The poor angular resolution of the HI distribution has prevented any detailed comparison with our data but we note that, although the HI distribution has a central depression (van Woerden et al. 1993), the average gas surface density rises again in the region under study to a value of 0.9 $M_{\odot}pc^{-2}$.

### *3.4. The dust patches*

The images reveal several dust patches close to the center. The presence of dust is not unusual in early-type galaxies and S0 galaxies (Kormendy and Djorgovski 1989) and has been specifically reported in the outer parts of NGC 5102 (Danks et al. 1979). The HST angular resolution is now known to enhance the detection capability of dust lanes close to the center of early-type galaxies (Van Dokkum and Franx 1995). The dust patches are best seen in the F342W image where the larger number of counts allows a better contrast. The three most prominent are found at position angles of 45°, 88° and 195°, and at distances of 2.″75, 1.″2 and 2.″2 respectively from the center of the galaxy. They do not form a particular pattern and have themselves irregular shapes with typical sizes of 0.″2. The first one noted above is found to extend in a sort of fainter ring shape. The third one merges into a larger and fainter structure at the edge of the FOC field that is possibly the inner part of the dust lane reported at 3″

and position angle 200° by Danks et al. (1979). In this third dust patch we evaluate an average extinction (for the F342W filter) of $\sim 1$ mag (i.e. a color excess E(B−V) of $\sim 0.2$) by comparison of light profiles on and off the absorbed area. The same type of measurement with the F175W image shows that the count rate right in the patch is not significantly different from the detector dark current, preventing even a crude determination of the extinction in the UV and therefore any constraint on the extinction law at UV wavelength.

## 4. Discussion

### *4.1. The nature of the resolved blue stars*

The data, as displayed in the CMD of Fig. 2, have been compared with the isochrones of Bertelli et al. (1994) for the initial chemical composition [Z = 0.02, Y = 0.28]. The absolute visual magnitude and effective temperature at different steps along these isochrones have been transformed in the $m_{175}$ vs. $m_{175}-m_{342}$ plane, using the *synphot* synthetic photometry package and the stellar atmosphere models of Kurucz (1979). A distance modulus of 27.47 and a foreground extinction with E(B−V) = 0.05 have been adopted (McMillan et al. 1994). Specifically, the isochrones for the ages $\log t$ = 6.6, 7.0, 7.2, 7.4, 7.6 and 7.8 years have been superposed on the data of Fig. 2. For a more familiar comparison, typical BOV and B5V stars would have $m_{175}-m_{342}$ colors of $\sim -1.7$ and $\sim -1.15$ respectively (along the $\log t$ = 6.6 isochrone).

Most of the blue stars detected and plotted in the CMD lie below the isochrone $\log t = 7.2$ and therefore appear as resulting from a recent star formation episode that, unless the IMF is truncated at high masses, would have ended $\sim 1.5 \times 10^7$ years ago. By comparison with the masses given along the isochrones, we determine that a truncation at $\sim 15$ $M_\odot$ would be necessary to mimic the observed CMD with on-going star formation and this possibility is discarded. There is, however, a difficulty with the recent star formation interpretation in the sense that the stars are expected to be more concentrated on the blue part of the isochrones: for the ages under consideration, the red part of the isochrones (color $> -1.1$) correspond to stars that are both massive (typically 13 $M_\odot$ for $\log t$ = 7.2) and in a relatively narrow range of mass; two reasons for a smaller proportion of stars along the red part than along the blue part of the isochrones. There are several possible explanations, including an unusual IMF, the effects of dust extinction, photometric errors and the presence of another type of blue stars than young stars.

For one, a dust extinction with a color excess E(B−V) = 0.1, as may be possible given the presence of dust patches, would move a star in the CMD by 0.23 mag to the red (the calculations were made with synphot assuming a galactic reddening law). Such a shift would increase the photometric dispersion that we may consider as illustrated by the data at the left of the main sequence but does not provide a satisfying explanation. We have explored the possibility of a systematic error which would affect the photometry in the F342W image. The crowding is more severe and the background higher in this latter image than in the F175W image. The trend in the CMD is not found to be changed by visually selecting only high quality data.

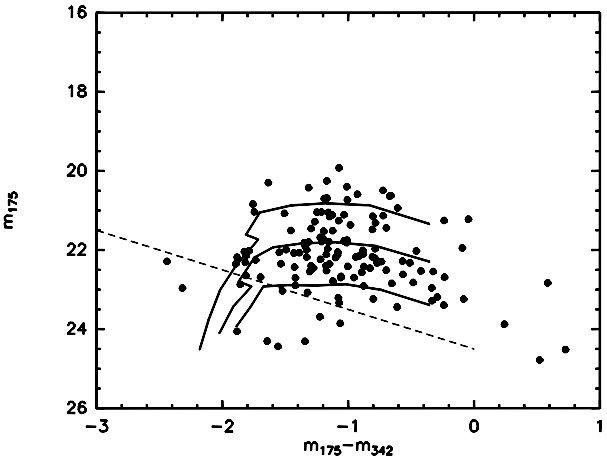


**Fig. 7.** Same as Fig. 2. The solid lines show the P-AGB evolutionary tracks of Vassiliadis & Wood for the core masses 0.900, 0.677, 0.569 $M_\odot$ (from top to bottom). The discontinuity in two of these tracks is due to the use of black body curves in place of stellar atmosphere models at high effective temperatures.

A last possibility is that we have resolved Post-Asymptotic Giant Branch (P-AGB) stars. The P-AGB stars are known to be the most UV luminous of the various hot and low-mass stars that can be anticipated in an old population (e.g. Greggio & Renzini 1990, Dorman et al. 1995). The stellar population responsible for the bulk of the visible light of the bulge is old enough to include P-AGB stars since a number of planetary nebulae have indeed been identified by McMillan et al. (1994). We have therefore superposed the recent evolutionary tracks for P-AGB stars of Vassiliadis & Wood (1994) on the data in Fig. 7. Specifically we have used the H-burning PNN evolutionary models for core masses of 0.569, 0.677 and 0.900 M⊙ and metallicity Z = 0.016. For transporting the tracks into the $m_{175}$ vs. $m_{175}-m_{342}$ plane, we have proceeded as previously, except that we have used bolometric corrections since we started from bolometric luminosities, and black-body curves when the effective temperatures are larger than encompassed by Kurucz's models. Fig. 7 shows that the blue stars may be P-AGB stars and not young stars. However, an interpretation exclusively in terms of P-AGB stars has difficulty in the sense that the distribution and relative proportion of the stars in the color-magnitude diagram do not match the time evolution pattern on the P-AGB tracks. First, the stars appear concentrated on the red part of the evolutionary tracks while time evolution is slower at high temperature; it has been verified that the lack of very blue objects does not result from a selection effect (the F342W frame is deep enough). Second, the time evolution strongly decreases when the stellar core-mass decreases (i.e. from upper to lower tracks) and would give a lower proportion of bright stars. A related argument is that a number of the resolved stars are too bright to be P-AGB stars.

It is also interesting to attempt a direct comparison with the number of P-AGB stars detected in an UV image of the bulge of

M31 (King et al. 1992). A limit of $m_{175} = 22.5$ in NGC 5102 is equivalent to a magnitude of 19.75 in M31 (adopting $\mu = 24.25$ and a color excess E(B−V) = 0.11 for the latter galaxy). The ∼30 stars brighter than this latter limit in M31 would imply ∼10 P-AGB stars in NGC 5102 after accounting for the respective bolometric luminosity of the two galaxies (i.e. the V luminosity assuming similar bolometric correction), in the fields of view observed in the ultraviolet. This number confirms the fact that most of the resolved stars are not P-AGB stars but it should be kept in mind that the comparison has many uncertainties since the origin of the UV flux from old population is not well understood and governed by metallicity effects.

In conclusion, and although the observed CMD is not fully understood, the resolved blue stars are most likely young stars and the last generation of a star formation episode that ended $\sim 1.5 \times 10^7$ years ago. It is somewhat ironic to see that the resolution of stars and the building of a CMD do not significantly improve the reliability of the interpretation over the previous arguments based on the integrated light, such as blue color, color gradient in the center and A-type Balmer absorption-lines in the spectrum (Faber et al. unpublished quoted by Burstein et al. 1988).

In the context of the favoured interpretation in terms of recently formed stars, we have examined how the determination of $\sim 1.5 \times 10^7$ years as the end of the star formation episode may be affected by the uncertainties of the measurements and the parameters used. A metallicity less than the solar abundance adopted, as suggested from the $Mg_2$ index of NGC 5102 (Burstein et al. 1988), would change the isochrones by a quantity smaller than the uncertainty of the determination itself ($\sim 0.3 \times 10^7$ years). This same uncertainty is also found larger than the difference between the two sets of isochrones (at specifically log t = 7.2) currently used for modeling of stellar populations (those of Bertelli et al. and those derived from the evolutionary tracks of Schaller et al. 1992). Last, the impact of a change of distance modulus (+0.16, −0.25 is the uncertainty quoted by McMillan et al. 1994) or of a systematic photometric error (about 0.2 mag) are readily seen in Fig. 2: again they stay within the accuracy of the determination of the end of the star formation episode.

A rough evaluation of the recent star formation rate is possible by counting the number of stars between two isochrones. We count 29 stars brighter than $m_{175} = 22$ between the log t = 7.4 and 7.2 isochrones. After a rough correction for completeness in our central domain, we get a number of ≈ 32. According to the distribution of masses along these isochrones (Bertelli et al. 1994), these stars have masses larger than $\sim 8\ M_\odot$. According to a Salpeter IMF, $1\ M_\odot$ formed corresponds to $7.4 \times 10^{-3}$ star more massive than $8\ M_\odot$. From our count of 32 stars over a period of about 9 Myr we therefore derive a star formation rate of $4.7 \times 10^{-4}\ M_\odot\ yr^{-1}$ in the FOC field of view.

### *4.2. The star formation history*

Because of the limit of detection and completeness effects, the resolved stars and the CMD cannot be used for determining when the star formation episode began? To address this question we have to rely on the integrated light, using specifically the IUE spectrum and the UV−V color.

We have a first qualitative indication that a large fraction of the star formation is not recent from the blueish $m_{175}-m_{342}$ integrated light in our FOC images (as discussed above Sect. 3.2) as compared to the color of resolved stars. It is also clear from evolutionary models (e.g. Fioc & Rocca-Volmerange 1997), that the star formation episode started a relatively long time ago. In these models, the combination of a relatively young burst to a conventional old population would never reproduce the relatively flat UV spectrum observed with IUE (Burstein et al. 1988). Unless we have special circumstances in NGC 5102 (extinction law, etc), we need to add the contribution of a spectrum declining in the UV as produced by an intermediate-age burst (500–1000 Myr). Fig. 8 shows a possible fit of the observed UV spectrum and the V magnitude in the IUE equivalent aperture with an intermediate-age burst of 800 Myr, an old population of 13 Gyr, and a young burst of 30 Myr (accounting for the young stars that we resolve). The spectral evolution models are from Fioc & Rocca-Volmerange (1997). In the example displayed in Fig. 8 the intermediate-age burst contributes to 60% of the light at 3200 Å but slightly different contributions and ages (in the range 500–800 Myr) are possible. The old component does not contribute significantly below 3000 Å indicating that our conclusions do not depend on the assumptions adopted for the UV spectrum and the star formation history of the old population.

A model with two instantaneous bursts has been used for simplicity but the intermediate-age burst has not necessarily ended abruptly and may naturally be seen as the beginning of a continuous star formation episode of which we are resolving the last generation of stars. A continuous formation would have the advantage to reduce the UV excess produced by the young burst at the shortest UV wavelengths (Fig. 8). In a continuous formation scenario, the star formation rate would be declining as a function of time if one wants the first generation of stars to be able to balance the last generation in terms of UV emission. A continuous exponentially decaying burst would imply a time constant of ≈ 70 Myr. Our result is close to the conclusion reached by Bica (1988) that the bulk of the star burst was formed between the ages 300 to 500 Myr.

### *4.3. Comparison with NGC 3115*

NGC 5102 has been compared with another S0 galaxy, NGC 3115, more typical of early-type galaxies than NGC 5102 in the sense that it is gas poor, exhibits a regular UV spectrum and fits well in the (1550−V) vs. $Mg_2$ absorption-line index relation for elliptical galaxies (Burstein et al. 1988, Bertola et al. 1993). The UV spectra of these two galaxies were also compared by Rocca-Volmerange & Guiderdoni (1987). A FOC exposure of NGC 3115 with the F175W filter and the same exposure time as the NGC 5102 image does not resolve any star. With a distance modulus of 30.21 (Elson 1997) and a foreground extinction $A_B = 0.10$ (Burstein & Heiles 1984), the isochrones and evolutionary paths for NGC 3115 are basically those of Figs. 2 and 7 translated down by 2.5 mag along the $m_{175}$ axis (ignoring

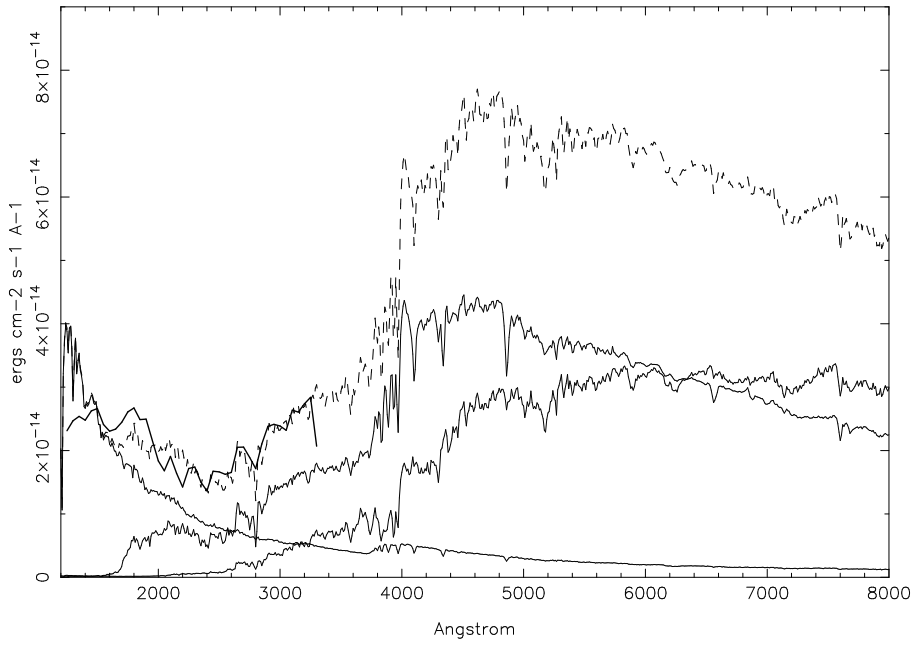


**Fig. 8.** Comparison of the IUE spectrum (thick solid line) (Burstein et al. 1988) with a synthetic spectrum (dashed line) resulting from the combination of an old population of 13 Gyr, an intermediate-age burst of 500 Myr, and a young burst of 30 Myr. Each of these components, listed in order of increasing UV flux at 2000 Å, is displayed as thin line.

the small effect on the color due to the assumption of a lower extinction). The following results stand out for NGC 3115: (i) stars earlier than approximately B0V are ruled out. If we assume a conventional IMF any star formation more recent than $\approx$ 15 Myr is excluded. (ii) the most massive P-AGB stars are below the detection threshold.

In conclusion, the constraints that UV imaging with the FOC can place on residual star formation in elliptical-type population are weak at the distance of most elliptical galaxies.

### *4.4. Interpretation*

The star formation phenomenon in the central region of the S0 galaxy NGC 5102 appears different from what we are used to in regular sites of star formation, in the sense that the young stars approximately follow the overall light distribution, do not seem confined to a disk and are not significantly clumped into clusters. These features as well as the existence of an UV gradient close to the center are naturally explained by the role of the galaxy potential well. Interestingly, the high angular resolution of the HST shows that, in contrast to the conclusion from ground-based observations (Pritchet 1979), the nucleus does not contribute to the UV gradient confirming that we have a purely stellar population phenomenon. The star formation also provides a natural explanation, at the expected location in the bulge, for the ring of ionized gas discovered by McMillan et al. (1994). According to the models of Leitherer & Heckman (1995), the total kinematic energy of $\sim 10^{52}$ ergs that McMillan et al. have calculated for the supershell would be produced over a time scale of 15 Myr by the last 2 Myr of the current star formation rate of $\sim 5 \times 10^{-4}$ $M_\odot$ yr$^{-1}$ (except for an IMF poor in massive stars).

Pritchet (1979), van Woerden et al. (1993) have searched for external factors that may have been able to supply gas and/or to trigger star formation in NGC 5102; they found no evidence for any possible encounter with another galaxy within the last few $10^9$ years. With the mounting evidence for a multiplicity of star formation history in early-type galaxies (Bressan et al. 1996) and especially the S0 galaxies (Fisher et al. 1996), the need for an external cause is less compelling. NGC 5102 would then only appear as an extreme example of a current phenomenon with perhaps the youth of the burst and the rather short distance favouring the detection of the residual star formation. This is also consistent with the fact that the star formation takes place in the center where the gas is expected to concentrate. The central depression in the HI distribution would be the witness of the star burst started 500–800 Myr ago that would have stopped because of gas exhaustion. The HI surface density of 0.9 $M_\odot pc^{-2}$ (van Woerden et al. 1993) is indeed at the lowest extremity of the range of threshold values reported by Kennicutt (1989). The very central peak of HI may indicate a new replenishment of gas since the end of the burst. This is highly speculative since the origin of the gas itself (not to mention the time scale of the processes involved) is not understood. In addition, even if the gas shed by stellar evolution is a possibility that could be invoked for the origin of the gas, it is not clear why the gas should be removed and/or the star formation inhibited in a number of early-type galaxies. In this context it is interesting to note the evidence of multiple episodes of star formation in local group dwarf ellipticals (Ferguson & Binggeli 1994) and the larger fraction of color gradient (bluer toward the center) among early-type dwarf galaxies (Vader et al. 1988, Chaboyer 1994) indicating a possible increase of the occurrence of relatively recent star formation in galaxies of low-luminosity. Although not a dwarf galaxy itself, NGC 5102 has a low luminosity ($M_B = -17.6$).

Finally our observations illustrate the general difficulty of understanding the nature of the stars responsible for the ultraviolet flux of elliptical galaxies, and, more specifically, of how any residual star formation may be distinguished from extreme hor-

izontal branch stars and their evolutionary progeny. The comparison with NGC 3115 shows that only the most massive stars (implying only very recent bursts or on-going star formation) can be resolved by the HST provided the ellipticals are not too distant. Even though blue stars are resolved, it may be difficult to determine individually the nature of these stars with UV photometry alone as shown by the example of NGC 5102. It is worth noting that other features or parameters such as blue color gradient or integrated UV−visible color are not free of ambiguities as indicators of star formation: globular clusters also have central UV color gradient (Djorgovski & Piotto 1992) and NGC 5102, although distinct from elliptical galaxies in the (15−V) vs. $Mg_2$ plane (Dorman et al. 1995), is at the location of the globular clusters in this plane.

## 5. Conclusion

A number of blue stars have been resolved within $\sim 3''$ from the center of NGC 5102, using the FOC with the F175W and F342W filters on board the *Hubble Space Telescope*. The main findings are.

– The angular resolution of the HST confirms and extends the previous ground-based result of a blue color gradient in the central region of the galaxy. The $m_{175}-m_{342}$ color gradient gets stronger at galactocentric distances smaller than $1''.4$ (21 pc) with the UV color decreasing from 0.0 to −0.5 at $0''.4$ (6 pc). This gradient does not continue in the nucleus which has a color similar to that found at a few arcsec in the inner bulge. The light profiles through both filters rise steeply at the resolution limit and show no evidence of a core.

– The resolved stars follow approximately the integrated light distribution with an indication that the stars are slightly more concentrated. There is no significant clustering and the stars do not seem to be confined to a disk.

– In the $m_{175}$ vs. $m_{175}-m_{342}$ color-magnitude diagram most of the resolved stars lie at positions where they may be interpreted either as young stars or as P-AGB stars. Both interpretations have difficulties. From the overall distribution in the color-magnitude diagram it seems more likely that the majority of the stars are young and can be explained as the result of a star formation episode that ended some 15 Myr ago.

– If the latter interpretation is correct, spectral evolutionary models show that this star formation episode began 500–800 Myr ago.

*Acknowledgements.* We thank R. Elson for communicating her results on the distance of NGC 3115 in advance of publication.

## References

Bertelli G., Bressan A., Chiosi C., Fagotto F., Nasi E., 1994, A&AS 106, 275
Bertola, F., Burstein, D., Buson, L. M., Renzini, A., 1993, ApJ 403, 577
Bica E., 1987, A&A 195, 76
Bressan A., Chiosi C., Tantalo R., 1996, A&A 311, 425
Brown T. M., Ferguson H. C., Davidsen, A. F., 1995, ApJ 454, L15
Burstein D., Heiles C., 1984, ApJS 54, 33
Burstein D., Bertola F., Buson L. M., Faber S. M., Lauer T. R., 1988, ApJ, 328, 440
Chaboyer B., 1994, In: Meylan G. & Prugniel P. (eds.) ESO/OHP Workshop on Dwarf Galaxies, p. 485
Danks A. C., Laustsen S., van Woerden H., 1979, A&A 73, 247
Djorgovski S., Piotto G., 1992, AJ 104, 2112
Dorman B., Rood R. T., O'Connell R. W., 1993, ApJ 419, 596
Dorman B., O'Connell R. W., Rood R. T., 1995, ApJ 442, 105
Elson R., 1997, MNRAS 286, 771
Ferguson H. C., Davidsen A. F., Kriss G. A. et al., 1991, ApJ 382, L69
Ferguson H. C., Davidsen A. F., 1993, ApJ 408, 92
Ferguson H. C., Binggeli B., 1994, A&AR 6, 67
Fioc M., Rocca-Volmerange B., 1997, A&A submitted
Fisher D., Franx M., Illingworth G., 1996, ApJ 459, 110
Greggio L., Renzini A., 1990, ApJ 364, 35
Jedrzejewski R. I., Hartig G., Jakobsen P., Crocker J. H., Ford H., 1994, ApJ 435, L7
Kennicutt R. C., 1989, ApJ 344, 685
King I. R., Deharveng J.-M., Albrecht R. et al., 1992, ApJ 397, L35
Kormendy J., Djorgovski S., 1989, ARA&A 27, 235
Kurucz R. L., 1979, ApJS 40, 1
Lauer T. R. et al., 1995, AJ 110, 2622
Leitherer C., Heckman T. M., 1995, ApJS 96, 9
McMillan R., Ciardullo R., Jacoby G. H., 1994, AJ 108, 1610
Nota A., Jedrzejewski R., Hack W., 1995, Faint Object Camera Instrument Handbook [Post-Costar], version 6.0 (Baltimore: STScI)
Paresce F., De Marchi G., Jedrzejewski, R. I., 1995, ApJ 442, L57
Pritchet C. J., 1979, ApJ 231, 354
Rocca-Volmerange B., Guiderdoni B., 1987, A&A 175, 15
Schaller G., Schaerer D., Meynet G., Maeder A., 1992, A&AS 96, 269
Vader J. P., Vigroux L., Lachièze-Rey M., Souviron J., 1988, A&A 203, 217
van den Bergh S., 1976, AJ 81, 795
van Dokkum P. G., Franx M., 1995, AJ 110, 2027
van Woerden H., van Driel W., Braun R., Rots A. H., 1993, A&A 269, 15
Vassiliadis E., Wood P. R., 1994, ApJS 92, 125

This article was processed by the author using Springer-Verlag TEX A&A macro package version 3.